

## REACTIVE RED 3 AND DIRECT BROWN 95 DYES ADSORPTION ONTO CHITOSAN

MAURUSA-ELENA IGNAT, VIORICA DULMAN,\* TINCA ONOFREI\*

*Centre of Advanced Research in Nanobioconjugates and Biopolymers,  
"Petru Poni" Institute of Macromolecular Chemistry, 41 A, Gr. Ghica Voda Alley,  
Iasi 700487, Romania*

*\*Department of Chemistry, "Alexandru Ioan Cuza" University, 11, Carol I Blvd.,  
Iasi 700506, Romania*

Received March 6, 2012

The chitosan availability in adsorption of C.I. Reactive Red 3-18159 (RR-3) and C.I. Direct Brown 95-30145 (DB-95) dyes from aqueous solutions was investigated by using the batch method. Experiments were carried out as a function of contact time, dye concentrations and temperature. The influence of pH and sodium chloride concentration were also investigated. The adsorption parameters were determined based on Langmuir and Freundlich isotherms obtained from the equilibrium adsorption data for the reactive dye and for the direct dye, while the kinetic and thermodynamic parameters were used to establish the adsorption mechanism. As an adsorbent, chitosan was found to prefer the RR-3 dye, retaining up to 151.52 mg textile dye per gram at 20 °C, whereas a retention of only 41.84 mg textile dye per gram at 50 °C has been achieved for DB-95 dye.

**Keywords:** adsorption isotherm, adsorption kinetics, chitosan, direct dye, reactive dye

### INTRODUCTION

The presence of synthetic textile dyes in industrial aqueous effluents causes serious environment pollution, because most of them are recalcitrant, toxic and highly resistant to degradation compounds. This is why, the efficient treatment of such industrial wastewaters is currently in real demand.<sup>1-3</sup>

The adsorption process has been considered one of the most efficient methods for removing dye pollutants from wastewater. The use of activated carbon as adsorbent for dyes is an efficient solution, but its cost is still a major disadvantage. A convenient alternative for decolorising wastewaters consists in the use of non-conventional adsorbents with lower cost and high efficiency, like natural biopolymers.<sup>4</sup> A derivative of chitin, chitosan, appears to be more attractive, since chitin is a biopolymer that is naturally available in abundance. Chitosan can be obtained by the deacetylation of chitin and due to its unique molecular structure (high contents of amino and hydroxyl functional groups) it has a high affinity for many classes of dyes. Chitosan has drawn particular attention due to its efficiency

as biosorbent and to its low cost compared to activated carbon.

A considerable number of studies report the results obtained in the use of chitosan and its grafted and crosslinked derivatives for removing dyes from aqueous solutions.<sup>5-10</sup> The biosorption performance of chitosan and its derivatives is influenced by several parameters, such as chitosan characteristics, process variables, dye chemistry and the solution conditions used in the study. The effectiveness of chitosan also depends on the natural source from which it has been obtained and on its form (gels, flakes, powders, particles).

Reactive dyes have come to be of interest since they may cause serious environmental problems. A remarkable performance achieved for certain types of chitosan has been reported, for example, crosslinked chitosan beads have an adsorption capacity in the range 1640- 2480 mg g<sup>-1</sup> for various reactive dyes.<sup>5</sup> Nawi *et al.*<sup>11</sup> immobilized chitosan on glass plates and obtained a maximum adsorption capacity of 172.41 mg g<sup>-1</sup> for Reactive Red 4. Guibal *et al.* Remark an

interesting interaction between chitosan and Reactive Black 5 dye, as to the sorption of the dye on solid chitosan using sulphuric acid for pH control.<sup>12</sup> Also, when using chitosan flakes as adsorbent for Reactive Red dye and Reactive Blue dye, the adsorption capacity achieved was of 22.48 mg·g<sup>-1</sup> and 70.08 mg·g<sup>-1</sup>, respectively.<sup>13</sup> Szygula *et al.*<sup>14</sup> used chitosan in a dissolved state in coagulation–flocculation processes for the removal of certain dyes from acidic solutions and observed that Reactive Black 5 required a short time to settle down. The investigation of the dynamic sorption of Reactive Black 5 onto chitosan showed that the adsorption efficiency and elution efficiency were always higher than 80% in each cycle.<sup>15</sup> Crosslinked chitosan with glutaraldehyde in the presence of magnetite was chemically modified to chitosan/amino resin and chitosan bearing both amine and quaternary ammonium chloride moieties, respectively. The uptake of Reactive Black 5 from aqueous solutions using both resins was studied and showed high affinity for the adsorption of reactive dye.<sup>16</sup> The chitosan-graft poly(methylmethacrylate) was found a much more efficient adsorbent than the parent chitosan for three anionic azo dyes (Procion Yellow MX, Remazol Brilliant Violet and Reactive Blue H5G) over a wide pH range of 4-10, the best results being achieved at pH 7.<sup>17</sup>

The number of studies devoted to direct dye adsorption is small, compared to the papers about reactive dyes. Direct Blue 78 dye removal from textile wastewater, using chitosan was studied.<sup>18</sup> the adsorption of Direct Red 23 dye and Acid Green 25 dye in single and binary systems was found to follow the Tempkin isotherm and the adsorption kinetics to conform to a pseudo-second-order model. The main characteristics of the composites made from chitosan and zinc oxide nanoparticles (biocompatibility, low cost

and eco-friendliness) strongly recommend these adsorbents as a suitable alternative for the elimination of Direct Blue 78 from aqueous solutions.<sup>19</sup> The adsorption/desorption behavior of different adsorbents and dyes in aqueous solutions was studied.<sup>20</sup> The preparation and characterization of a new s-IPN composite hydrogel, based on polyacrylamide and chitosan, and its interaction with Direct Blue 1 dye were also reported.<sup>21</sup>

The present paper describes the adsorption behavior of Reactive Red 3 (RR-3) dye and Direct Brown 95 (DB-95) dye towards chitosan. The influence of some factors, such as pH, dye concentration, contact time, temperature and concentration of sodium chloride, on chitosan adsorption capacity for the two dyes, has been investigated. The kinetics and thermodynamic parameters that characterize the adsorption processes were estimated. It has been noted that the two dyes in the study were not mentioned in literature, as far as the possibility of their removal with chitosan and its derivatives is concerned.

## EXPERIMENTAL

### Materials and methods

#### Chitosan

Chitosan (CH-69) with an acetylation degree of 34% and a relative molecular weight (g mol<sup>-1</sup>) of 350000 was obtained from Vanson Co., Canada. The chitosan flakes were ground and sieved to 100-150 mesh diameter. The structure of the used adsorbent is shown in Figure 1a.

#### Dyes

Two commercial dyes, C.I. Reactive Red 3-18159 (RR-3) and C.I. Direct Brown 95-30145 (DB-95), whose structures are shown in Figure 1b and c, were purchased from the Faculty of Textiles – Leather and Industrial Management, Iasi, Romania, in the form of sulphonic acid salts, which determines their solubility in water.

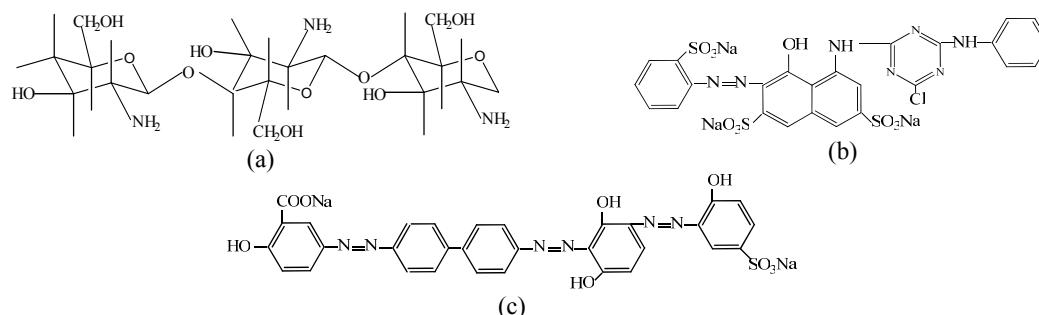


Figure 1: The chemical structure of chitosan (a), C.I. Reactive Red 3-18159 dye (RR-3) (b) and C.I. Direct Brown 95-30145 dye (DB-95) (c)

DB-95 direct dye has one sulphonic group and RR-3 reactive dye has three sulphonic groups, their molecular weights ( $\text{g mol}^{-1}$ ) being of 774 and 602, respectively. Aqueous solutions of  $1000 \text{ mg L}^{-1}$  textile dye (used without preliminary purification) were prepared using double-distilled water and then diluted when necessary. The aqueous dye solution with an initial concentration of  $100 \text{ mg L}^{-1}$  had an initial pH of 5.15 for RR-3 dye and 6.06 for DB-95 dye.

### Adsorption kinetics

Adsorption kinetics experiments were carried out using the batch method. The effect of contact time on the removal of both dyes was followed by shaking (on a rotating shaker) an aqueous dye solution without pH correction ( $100 \text{ mL}$ ) of known concentration, into which  $0.12 \text{ g}$  chitosan at a constant temperature ( $20 \text{ }^\circ\text{C}$ ) was introduced. The stirring speed was kept constant at  $400 \text{ rpm}$ . At predetermined intervals of time, the samples were taken and centrifuged at  $5000 \text{ rpm}$  for  $10$  minutes. The corresponding absorbance dye concentration left in the solution was measured spectrophotometrically with a UV-Vis 1700 Pharma Spec spectrophotometer (Shimadzu, Kyoto, Japan) at  $532 \text{ nm}$  for RR-3 and  $400 \text{ nm}$  for DB-95 dye. Then, the amount of the adsorbed dye at time  $t$ ,  $q_t$  ( $\text{mg g}^{-1}$ ) was determined by the following relation:

$$q_t = \frac{(C_0 - C_t)V}{w} \quad (1)$$

where  $C_0$  and  $C_t$  are the initial concentration and concentration at time  $t$  in the dye solution ( $\text{mg L}^{-1}$ ), respectively,  $V$  is the volume of solution ( $\text{L}$ ),  $w$  is the mass of adsorbent used ( $\text{g}$ ).

The equilibrium time established between chitosan and the dye solutions was subsequently used in the isotherm experiments.

### Equilibrium studies

The adsorption isotherms were obtained by employing  $0.03 \text{ g}$  of chitosan and  $25 \text{ mL}$  aqueous solution of dye with various concentrations. The solutions were stirred until they reached adsorption equilibrium and then the same procedure as that described above was followed. The tested temperatures were in the range  $20\text{-}50 \text{ }^\circ\text{C}$ .

The adsorption capacity of chitosan was evaluated by the amount of dye adsorbed at equilibrium by the relation:

$$q_e = \frac{(C_0 - C_e)V}{w} \quad (2)$$

where  $q_e$  is the amount of dye adsorbed per weight unit of adsorbent at equilibrium ( $\text{mg g}^{-1}$ ),  $C_0$  and  $C_e$  are the initial and equilibrium concentrations of dye in solution ( $\text{mg L}^{-1}$ ),  $V$  is the volume of solution ( $\text{L}$ ),  $w$  is the mass of adsorbent used ( $\text{g}$ ).

## RESULTS AND DISCUSSION

### Effect of contact time and initial dye concentration

The influence of contact time on the adsorption of both dyes onto chitosan from aqueous solutions with initial concentrations between  $20\text{-}100 \text{ mg L}^{-1}$  was observed under constant conditions, as those mentioned above. As shown in Figure 2 (a, b), dye adsorption is correlated with both the concentration of dyes and contact time. The contact time curves are smooth and continuous, leading to equilibrium. It is also obvious that the  $q_t$  value increases with the initial concentration of the two dyes and then tends to a plateau, when it can be assumed that there is a saturation of the adsorption sites on the adsorbent. Thus, the RR-3 dye at low concentration ( $20\text{-}30 \text{ mg L}^{-1}$ ) is quantitatively removed in  $45\text{-}50$  minutes. For the DB-95 dye, the time necessary to reach equilibrium is higher for the same concentrations ( $\sim 80$  minutes). The amount of retained dye did not change even if contact time was extended, which proves that saturation was reached, as mentioned above. Also a higher rate of adsorption for RR-3 on chitosan was noted.

### Kinetic models

The kinetic analysis of DR-95 and RR-3 adsorption onto chitosan was performed using the pseudo-first-order model proposed by Lagergreen,<sup>22</sup> pseudo-second-order model proposed by Ho and McKay,<sup>23</sup> the Elovich kinetic model<sup>24</sup> and the intraparticle diffusion model.<sup>25</sup>

The adsorption dynamics can be appreciated by determining the adsorption rate constant using a linear form of the Lagergreen equation (3).

$$\log(q_e - q_t) = \log q_e - \frac{k_1}{2.303} \cdot t \quad (3)$$

where  $q_e$  and  $q_t$  are the amounts of dye adsorbed ( $\text{mg g}^{-1}$ ) at equilibrium and at time  $t$ , respectively, and  $k_1$  is the rate constant.

The pseudo-first-order kinetics constant  $k_1$  ( $\text{min}^{-1}$ ) values were calculated from the slopes of the linear plot of  $\log(q_e - q_t)$  versus  $t$  and  $q_e$  corresponding model ( $q_{ec}$ ) from intercept (Figure 3a and b).

The linear form of the equation that describes the adsorption kinetics corresponding to the pseudo-second-order model is the following:

$$\frac{t}{q_t} = \frac{1}{k_2 q_e^2} + \frac{1}{q_e} t \quad (4)$$

where  $k_2$  is the rate constant of pseudo-second order ( $\text{g mg}^{-1} \text{min}^{-1}$ ).

The linear plot of  $t/q_t$  versus  $t$  allows the calculation of  $k_2$ ,  $q_{ec}$  values. Also, the initial adsorption rate  $h$  ( $\text{mg g}^{-1} \text{min}^{-1}$ ) can be obtained by:

$$h = k_2 q_e^2 \quad (5)$$

Elovich equation has been used to interpret the kinetics of adsorption. It has been found useful in describing the predominantly chemical adsorption on highly heterogeneous adsorbents. The linear form of Elovich equation is given by:

$$q_t = \frac{1}{\beta} \ln(\alpha\beta) + \frac{1}{\beta} \ln t \quad (6)$$

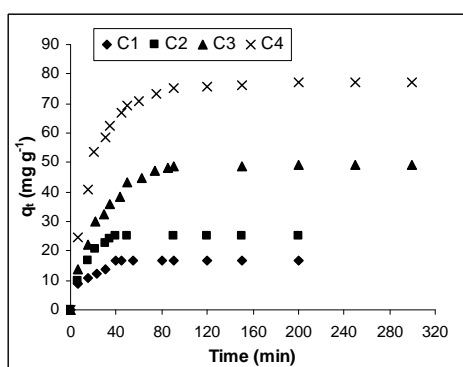
where  $\alpha$  represents the initial adsorption rate ( $\text{mg g}^{-1} \text{min}^{-1}$ ) and the  $\beta$  is related to the extent of surface coverage and activation energy for chemisorption ( $\text{g mg}^{-1}$ ). Elovich parameters  $\alpha$  and

$\beta$  could be computed from the plots of  $q_t$  versus  $\ln t$ .

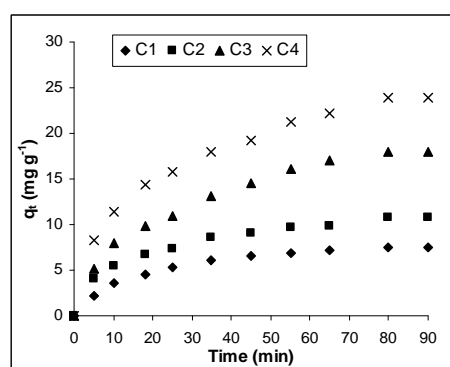
Table 1 shows that the values of the determination coefficients  $R^2$  of the pseudo-second-order model are all higher than those of the first-order model. The experimental data follow the linear relationship of pseudo-second-order adsorption model. By comparing the equilibrium concentration values determined experimentally ( $q_e$ ) with those calculated ( $q_{ec}$ ), a good agreement has been observed for RR-3 dye (Figure 3 c), but there are great differences for all concentrations of DB-95 dye. The  $k_2$  rate constants decreased with the increase in the initial dye concentration. For the smaller concentration of the dyes, maximum  $k_2$  values of  $2.2 \cdot 10^{-2} \text{ mg g}^{-1} \text{min}^{-1}$  were observed for DB-95 dye and of  $1.23 \cdot 10^{-3} \text{ mg g}^{-1} \text{min}^{-1}$  for RR-3 dye.

Table 1  
Kinetic parameters for RR-3 dye and DB-95 dye adsorption

$C_0$ , $\text{mg L}^{-1}$	$q_e$ , $\text{mg g}^{-1}$	Pseudo-first-order kinetic model			Pseudo-second-order kinetic model				Elovich model		
		$q_{ec}$ , $\text{mg g}^{-1}$	$k_1$ , $\text{min}^{-1}$	$R^2$	$q_{ec}$ , $\text{mg g}^{-1}$	$k_2$ , $\text{g mg}^{-1} \text{min}^{-1}$	$h$ , $\text{mg g}^{-1} \text{min}^{-1}$	$R^2$	$\alpha$ , $\text{mg g}^{-1} \text{min}^{-1}$	$\beta$ , $\text{g mg}^{-1}$	$R^2$
RR-3 dye											
20	16.72	11.09	0.0082	0.959	17.39	0.00123	0.36	0.997	11.11	0.192	0.974
30	25.25	25.87	0.0762	0.977	26.25	0.00034	0.232	0.998	22.45	0.114	0.996
60	49.00	43.13	0.0336	0.984	52.08	0.00010	0.41	0.997	46.12	0.069	0.990
100	81.43	60.95	0.0332	0.956	81.43	0.000022	0.18	0.999	55.43	0.051	0.967
DB-95 dye											
20	7.54	6.90	0.0449	0.993	8.97	0.02264	1.82	0.999	3.0533	0.519	0.996
30	10.77	8.45	0.0362	0.982	12.5	0.00788	1.23	0.996	3.4576	0.387	0.996
60	17.94	17.40	0.0410	0.975	22.07	0.00193	0.94	0.991	8.9662	0.214	0.984
100	23.89	20.34	0.0368	0.984	28.33	0.00078	0.62	0.994	9.3430	0.169	0.995



a)



b)

Figure 2: Effect of contact time and initial dye concentration for: a) RR-3 and b) DB-95 dyes (C1 – 20  $\text{mg L}^{-1}$ ; C2 – 30  $\text{mg L}^{-1}$ ; C3 – 60  $\text{mg L}^{-1}$ ; C4 – 100  $\text{mg L}^{-1}$ )

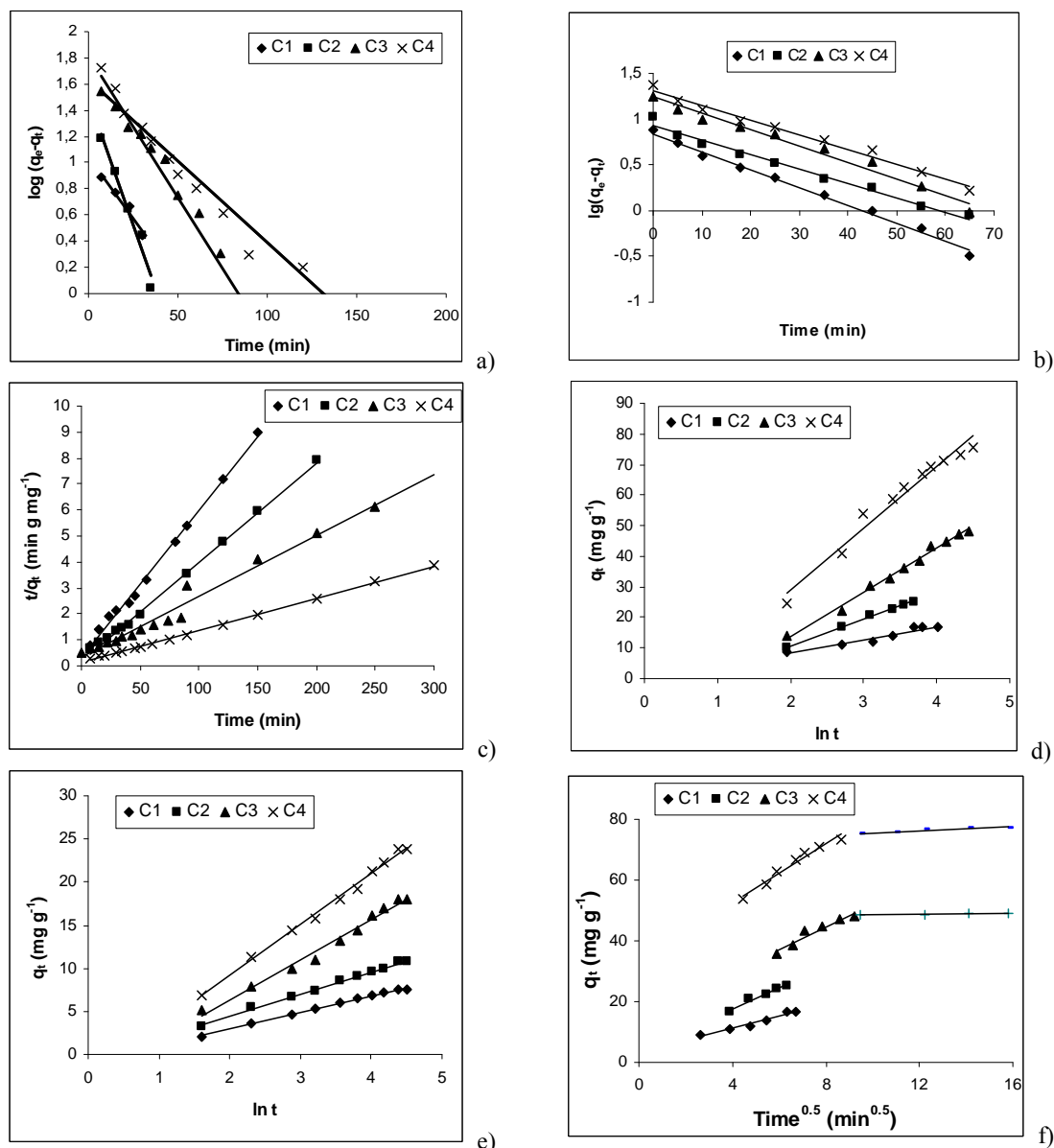


Figure 3: Pseudo-first-order kinetics (a) RR-3 dye, (b) DB-95 dye; pseudo-second-order kinetics (c) RR-3 dye; Elovich model (d) RR-3 dye, (e) DB-95 dye; and intraparticle diffusion model (f) RR-3 dye plots for the adsorption of dyes at various concentrations (C1 – 20 mg L<sup>-1</sup>; C2 – 30 mg L<sup>-1</sup>; C3 – 60 mg L<sup>-1</sup>; C4 – 100 mg L<sup>-1</sup>)

For the direct dye, although  $R^2$  values of the first-order model are lower than those of the model Ho,  $q_{ec}$  values for this model are estimated to be more accurate. The maximum  $k_f$  value for the adsorption of Direct Blue A dye by the same type of chitosan has been reported as  $3.74 \cdot 10^{-2} \text{ min}^{-1}$  for the same concentration.<sup>26</sup>

The Elovich model allows the assessment of heat of adsorbent-adsorbate interactions. Due to these interactions, the heat of adsorption of all molecules in the layer decreased linearly with the

increase of initial adsorption rate.<sup>27</sup> For the two dyes, it was noticed that  $\beta$  values decreased with the increase in the initial dye concentration, while the initial adsorption rate ( $\alpha$ ) increased under the same conditions (Table 1, Figure 3 d and e).

The mechanism of dye adsorption on chitosan is complex. It primarily involves the surface physical adsorption on biosorbent, but there exists the possibility of a covalent binding of dyes on the substrate that occurs simultaneously with the exchange process. At pH 6, only part of amine

groups will be protonated and will be available for electrostatic interaction.<sup>5</sup>

In general, dye adsorption on an adsorbent material may be assumed to involve four steps,<sup>5</sup> of which film diffusion (diffusion of dye through the boundary layer to the surface of the adsorbent) and pore diffusion or intraparticle diffusion (transport of the dye from the surface into the pores of the particle) are essential for establishing the mechanism.

The diffusion mechanism can be identified by using the intraparticle diffusion model proposed by Weber and Morris.<sup>25</sup>

$$q_t = k_{id} t^{0.5} + I \quad (7)$$

where  $k_{id}$  is the intraparticle diffusion rate constant ( $\text{mg g}^{-1} \text{min}^{-0.5}$ ) and  $I$  is the intercept ( $\text{mg g}^{-1}$ ).

If the rate-controlling step is an intraparticle diffusion, a plot of dye adsorbed ( $q_t$ ) against square root of contact time ( $t^{0.5}$ ) leads to a straight line passing through the origin.<sup>28</sup> When the plots do not pass through the origin, it is an indication of some degree of boundary layer control and of the fact that the intraparticle diffusion is not the only rate-limiting step. In this case, the adsorption process is complex and more kinetic models that

operate simultaneously may control the rate of dye adsorption.

The rate constants of intraparticle diffusion ( $k_{id}$ ) for both dyes were obtained from the linear part of the plots  $q_t$  vs.  $t^{1/2}$  for different concentrations of dyes (Table 3). In the range of initial dye concentration of 20-100  $\text{mg L}^{-1}$ , the values for  $k_{id1}$  increase with increasing dye concentration, which corresponds to an enhanced diffusion of dye molecules from the outer surface of the adsorbent into macropores. For initial concentrations between 60-100  $\text{mg L}^{-1}$  of RR-3 dye, two separate regions are found in the plot (Figure 3 c); namely, the first straight part can be attributed to the macropore diffusion (rate constant  $k_{id1}$ ) and the second linear portion to micropore diffusion (rate constant  $k_{id2}$ ). The values of intercept for RR-3 dye are higher than those for DB-95 dye, which shows a greater contribution to the surface adsorption in the rate-controlling step.

The determination coefficients  $R^2$  for the intraparticle diffusion model are lower than those for the pseudo-second-order model for RR-3 dye and for the pseudo-first-order model for DB-95 dye.

Table 2  
Intraparticle diffusion parameters for the removal of RR-3 and DB-95 at different initial dye concentrations

$C_0$ , $\text{mg L}^{-1}$	RR-3 dye						DB-95 dye		
	$k_{id1}$ , $\text{mg g}^{-1} \text{min}^{-0.5}$	$I_1$ , $\text{mg g}^{-1}$	$R^2$	$k_{id2}$ , $\text{mg g}^{-1} \text{min}^{-0.5}$	$I_2$ , $\text{mg g}^{-1}$	$R^2$	$k_{id2}$ , $\text{mg g}^{-1} \text{min}^{-0.5}$	$I_1$ , $\text{mg g}^{-1}$	$R^2$
20	2.05	3.04	0.9730	-	-	-	2.13	1.85	0.9767
30	3.38	4.10	0.9753	-	-	-	2.24	8.49	0.9765
60	3.73	14.82	0.9349	0.084	47.74	0.9273	3.96	9.80	0.9748
100	40.67	38.42	0.9460	0.33	72.32	0.9814	4.26	35.89	0.9773

Table 3  
Langmuir parameters at different temperatures for adsorption of RR-3 and DB-95 dyes

Temperature, K	$q_m$ , $\text{mg g}^{-1}$	$K_L$ , $\text{L g}^{-1}$	$b$ , $\text{L mg}^{-1}$	$R^2$	$R_L$
RR-3 dye					
293	151.52	2.52	0.01667	0.9838	0.833-0.231
303	120.23	2.08	0.01814	0.9805	0.821-0.216
313	106.38	1.69	0.01586	0.9865	0.840-0.240
DB-95 dye					
293	36.10	0.89	0.02469	0.9982	0.771-0.168
303	38.46	0.99	0.02647	0.9967	0.759-0.159
323	41.84	1.49	0.01138	0.9980	0.699-0.123

The different behavior of chitosan towards the two dyes can be correlated with their structure

and molecular weight, because they belong to distinct classes of dyes in terms of tinctorial

properties. Cheung *et al.*<sup>29</sup> have established that during acid dye adsorption onto chitosan, the mechanism was predominantly intraparticle diffusion, but there was also a dependence on pore size as the dye diffuses into macropores, mesopores and micropores, respectively.

### Adsorption isotherms

Generally, adsorption isotherms describe the way pollutants interact with the adsorbent materials, and thus are critical for the optimization of the adsorption mechanism pathways, emphasizing the surface and capacities of adsorbents and the effective design of the adsorption systems.<sup>30</sup>

#### Langmuir isotherm

Experimental data regarding the adsorption of dyes considered in the study on chitosan at different temperatures were analyzed by the Langmuir equation (8).<sup>31</sup>

$$q_e = \frac{K_L \cdot C_e}{1 + b \cdot C_e} \quad (8)$$

where  $K_L$  – Langmuir constant ( $L \text{ g}^{-1}$ );  $C_e$  – dye solution concentration at equilibrium ( $\text{mg L}^{-1}$ );  $q_e$  – the amount of retained dye ( $\text{mg g}^{-1}$  sorbent) at equilibrium;  $b$  – adsorption coefficient ( $L \text{ mg}^{-1}$ ).

A linearized form of equation (8) can be obtained as follows:

$$\frac{C_e}{q_e} = \frac{1}{K_L} + \frac{b \cdot C_e}{K_L} \quad (9)$$

A plot of  $C_e/q_e$  vs  $C_e$  leads to a straight line with the  $b/K_L$  slope and an intercept with an ordinate equal to  $K_L^{-1}$ . The  $q_m$  maximum capacity of adsorption ( $\text{mg dye g}^{-1}$  adsorbent) is computed by means of the relation:

$$K_L = q_m \cdot b \quad (10)$$

From the Langmuir plot for adsorption of both dyes at different temperatures, the Langmuir parameters were obtained (Table 3). A maximum adsorption capacity of chitosan of  $151.52 \text{ mg g}^{-1}$  for RR-3 reactive dye was reached at  $20 \text{ }^\circ\text{C}$ . The  $q_m$  and  $K_L$  values are shown to decrease when the temperature rises from  $20 \text{ }^\circ\text{C}$  to  $40 \text{ }^\circ\text{C}$ . The fact that the adsorption of RR-3 dye is not favored by increasing temperature indicates that the process is exothermic. The Langmuir isotherms obtained from experimental data of direct dye DB-95 adsorption on chitosan reflect the fact that increasing the temperature from  $20 \text{ }^\circ\text{C}$  to  $50 \text{ }^\circ\text{C}$  leads to  $q_m$  values from  $36.10$  to  $41.84 \text{ mg g}^{-1}$ . Simultaneously, the values of  $K_L$  are found to be intensified.

The essential characteristic trait of a Langmuir isotherm expressed in terms of a dimensionless separation factor ( $R_L$ ) can be computed by the relation:

$$R_L = \frac{1}{1 + bC_0} \quad (11)$$

The computed values of  $R_L$  (Table 3) in the range (0-1) confirmed that the adsorption behaviour of the chitosan adsorbent was favorable for both dyes.

There is also evidence of higher adsorbent affinity for the reactive dye. The different behavior of the same adsorbent towards the two dyes RR-3 and DB-95 under investigation belong to different classes in terms of tinctorial properties, have different structures and their maximum adsorption capacity is related to their chemical structure, to the dimensions of the dye organic chains and the number and positioning of the dye functional groups (Figure 1b,c).

In the dyeing process, generally for reactive dyes, covalent bonds between the reactive groups of the dye and the fiber are formed; namely -OH groups of cellulose fibers (cotton, viscose, flax, hemp) and -NH<sub>2</sub> or -OH groups of wool, silk, polyamide.<sup>32-34</sup> The retention of direct dye anions is due to the formation of hydrogen bonds and van der Waals forces with cellulose fibers favored by the coplanar structure of linear and direct dyes.<sup>32</sup>

#### Freundlich isotherm

The study of Freundlich isotherm was performed by the equation:

$$\log q_e = \log K_F + 1/n \log C_e \quad (12)$$

where  $q_e$  is the amount of adsorbed dye ( $\text{mg L}^{-1}$ ) at equilibrium;  $K_F$  and  $n$  are constants that reflect adsorption capacity and intensity of adsorption, respectively. The  $K_F$  and  $n$  constants were computed from the intercept and slope, respectively, of the linear plots for  $\log q_e$  vs.  $C_e$  (Table 4). The  $n$  values ranging between 1 and 10 indicate a favorable adsorption for both dyes.

#### Thermodynamics

For RR-3 dye the thermodynamic parameters of the adsorption process can be evaluated by using the van't Hoff equation with the values of  $K_L$  obtained at different temperatures:<sup>5,35</sup>

$$\log K_L = -\frac{\Delta H^0}{2.303RT} + \frac{\Delta S^0}{2.303R} \quad (13)$$

where  $\Delta H^0$  and  $\Delta S^0$  are enthalpy and entropy changes, respectively.  $R$  is the gas constant ( $8.314 \text{ J mol}^{-1} \text{ K}^{-1}$ ) and  $T$  is absolute temperature (K).

The dependence  $\log K_L$  versus  $1/T(\text{K})$  is represented in Figure 4, where the slope of the straight line is  $\Delta H^0/2.303R$ . The  $\Delta H^0$  value of  $-13.24 \text{ kJ mol}^{-1}$  for RR-3 dye was obtained. The negative value of this parameter indicates the heat releasing during adsorption and the exothermic nature of the process. From the intercept with ordinate ( $\Delta S^0/2.303R$ ) the negative value computed of  $\Delta S^0$  ( $-37.62 \text{ J K}^{-1} \text{ mol}^{-1}$ ) shows that the randomness at the solid chitosan–RR-3 dye solution interface decreases during the adsorption for the system under consideration.

The Gibbs free energy change ( $\Delta G^0$ ) was computed as follows:

$$\Delta G^0 = \Delta H^0 - T\Delta S^0 \quad (14)$$

For the range of temperature from 293K to 313K,  $\Delta G^0$  varies from  $-2.21$  to  $-1.46 \text{ kJ mol}^{-1}$ . The negative values of  $\Delta G^0$  confirm the feasibility of the process and the spontaneous nature of the adsorption of RR-3 dye onto chitosan. In addition, the considerably low  $\Delta G^0$  values illustrate the saturation in the adsorption process.<sup>36</sup> Nawi *et al.*<sup>11</sup> also reported a similar observation for the adsorption of Reactive Red 4 by immobilized chitosan on glass plates.

Table 4  
Freundlich isotherm constants at different temperatures

Temperature, K	$K_F$ , ( $\text{mg g}^{-1}$ )( $\text{L g}^{-1}$ ) <sup>n</sup>	n	R <sup>2</sup>
RR-3 dye			
293	3.62	1.37	0.9923
303	3.27	1.53	0.9976
313	2.73	1.43	0.9906
DB-95 dye			
293	1.96	1.71	0.9882
303	2.62	1.99	0.9859
323	3.31	2.04	0.9737

### Effect of pH

The initial pH of a dye solution is one of the most important parameters affecting the adsorption process because pH influences the chemistry of both chitosan adsorbent and dye molecules in an aqueous solution. The effect of pH on chitosan adsorption capacity was studied in the range 2.5–7.0 (acidity was corrected with solutions  $10^{-1}$ – $10^{-3} \text{ M H}_2\text{SO}_4$ ). Other mineral or organic acids cannot be used because chitosan is solubilised totally or partly.<sup>37,12</sup>

The changes in the adsorption of RR-3 and DB-95 dyes over a pH range of 2.5–7.0 on chitosan are depicted in Figure 5. For DB-95 it was observed that for a pH of 2.5 there were a lot of fine particles in suspension in the solution, which proves the instability of the dye in acidic solutions. This may be the reason that no adsorption occurred at this pH.

The quantities of the dye adsorbed increase with decreasing acidity, until a pH of 5.0 is reached for RR-3 dye and of 6.0 for DB-95 dye.

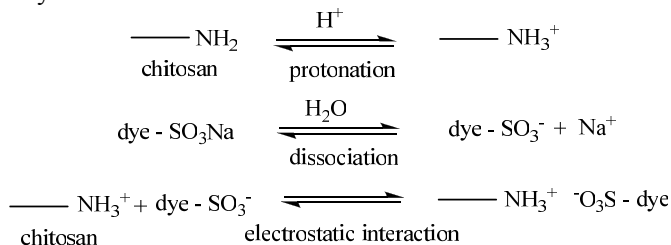
Above these values, the adsorption of dyes decreases with increasing pH. Also, one can see that under these experimental conditions, RR-3 dye retention is greater than that of DB-95 dye. The optimum pH reported for chitosan in the case of Reactive Red 4 was 6.0<sup>11</sup> and for Direct Red 23 was 2.0.<sup>18</sup>

From Figure 5, it may be observed that the final pH after the adsorption of both dyes increases for an initial pH range of 3.3–5.5. Sakkayawong *et al.*<sup>38</sup> also reported that the solution pH changes during RR141 reactive dye adsorption onto chitosan. The explanation for this is that under acidic conditions hydrogen ions in the solution could protonate the amine groups of the biopolymer and thus cause the increased pH.

The initial tests in the pH range of 8–11 led to results that show that a decrease in adsorption capacity can be attributed to a competition between the  $\text{OH}^-$  ions in basic medium and the anions of dyes for the positively charged adsorption sites, which could lead to a decrease of biosorption capacity.

The influence of pH in the adsorption processes is due to both the dye and chitosan. In aqueous solutions with different pH, dye dissociation occurs as a function of their acid-base characteristic traits. The strongly acidic sulphonate groups of the dyes were dissociated

and converted to anionic dye ions. At the same time, the chitosan in an acid medium undergoes protonation at nitrogen atoms, which favors the adsorption dye anion by ion exchange process according to the general equilibrium:<sup>5</sup>



The presence of carboxyl groups in DB-95 dye can contribute to the adsorption mechanism through the electrostatic interaction between COO<sup>-</sup> reactive groups of dye and protonated chitosan, but it should be noted that the involvement of strongly dissociated sulfonic groups is much higher than that of partially dissociated carboxyl groups. Also, it was observed that the two dyes contain different

numbers of groups (-OH, -NH-, -N=N-) that can participate at the formation of covalent, coulombic, hydrogen bonding or van der Waals forces.<sup>39</sup>

Crini and Badot<sup>5</sup> point out that the accessible amine groups in chitosan are in the main reactive groups for anionic dye adsorption, although hydroxyl groups (especially in the C-3 position) may contribute to adsorption.

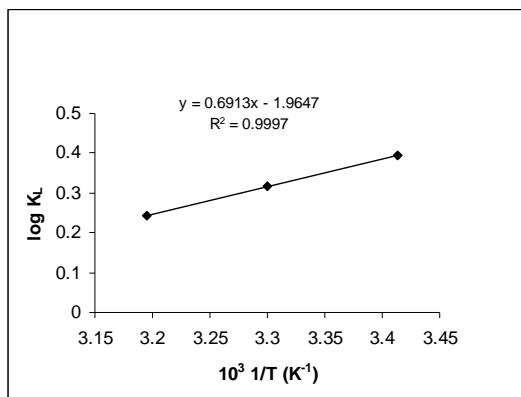


Figure 4: The dependence of log K<sub>L</sub> on 1/T (K<sup>-1</sup>) for RR-3 dye

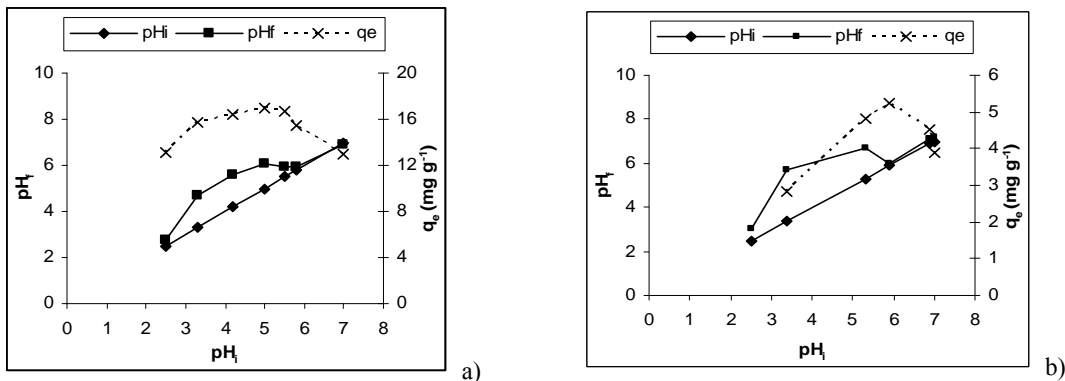


Figure 5: Effect of pH<sub>i</sub> on dye adsorption and variation of pH<sub>f</sub> after retention of a) RR-3 dye; b) DB-95 dye; (C<sub>0</sub> = 20 mg L<sup>-1</sup>; w = 0.03 g; V = 25 mL; 20 °C )

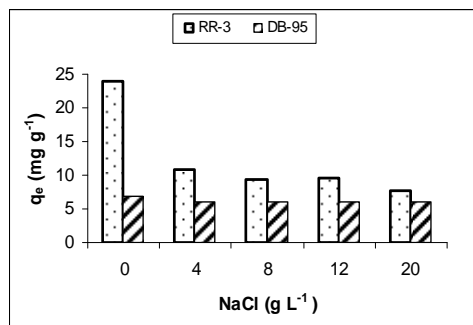


Figure 6: Effect of NaCl concentration on adsorption of RR-3 and DB-95 dyes on chitosan ( $C_0 = 27$  mg dye L<sup>-1</sup>;  $w = 0.03$  g;  $V = 25$  mL; 20 °C;  $t = 1$  hour)

### Effect of ionic strength

In typical dyeing systems, certain electrolytes are known to affect dye adsorption on fibers. Different concentrations of sodium chloride, between 4 and 20 g L<sup>-1</sup>, are observed to decrease the adsorption of both dyes on chitosan (Figure 6). In the case of RR-3, the effect of NaCl is much stronger, as compared to DB-95 dye. As the concentration of NaCl increased from 0 to 4 g L<sup>-1</sup>, the retained amount of RR-3 dye diminished to almost a half and then it remained constant, allowing the growth of electrolyte amount to 20 g L<sup>-1</sup>. A similar behavior was found by Gao *et al.*<sup>40</sup> for Acid Yellow 17 dye adsorbed on activated sludge. The author explained that in the presence of NaCl, the common ion effect of Na<sup>+</sup> caused a decrease of dye dissociation and, as a result, the dye biosorption on non-living aerobic granular sludge was reduced. In solution, this effect would reduce the electrostatic attraction force between R-NH<sub>3</sub><sup>+</sup> and Dye-SO<sub>3</sub><sup>-</sup>.

The same amount of NaCl reduced insignificantly the adsorption of direct dye DB-95. The adsorption capacities of the native or heat-treated fungal biomass to Direct Blue 1 and Direct Red 128 dyes were not significantly affected by increasing ionic strength (NaCl from 0 to 0.5 M).<sup>41</sup>

### CONCLUSIONS

The batch adsorption studies have shown that the adsorption of Reactive Red 3 and Direct Brown 95 dyes from aqueous solution is influenced by the contact time, initial dye concentration, pH, temperature and addition of sodium chloride. According to the experimental data, the adsorption processes follow a pseudo-second-order model for Reactive Red 3 and a pseudo-first-order one for Direct Brown 95 dye.

Furthermore, the Langmuir and Freundlich isotherm models fit with our results and could well describe the adsorption of these dyes onto chitosan. Intraparticle diffusion has an important role in the adsorption mechanism, together with ion-exchange mechanisms. Since temperature values influence the process as a function of the dye type, the maximum adsorptive capacity was determined to be of 151.52 mg g<sup>-1</sup> for Reactive Red 3 at 20 °C, and of 41.84 mg g<sup>-1</sup> for Direct Brown 95 at 50 °C, respectively. These results demonstrate that the adsorption of the two dyes on chitosan depends on their particular structure.

### REFERENCES

- S. J. Allen, B. Koumanova, *J. University of Chemical Technology and Metallurgy*, **40**, 175 (2005);
- G. Crini, *Bioresource Technol.*, **97**, 1061 (2006).
- V. K. Gupta, Suhas, *J. Environ. Manag.*, **90**, 2313 (2009).
- D. L. Michelsen, L. L. Fulk, R. M. Woodby, G. D. Boardman, in "A.C.S. Symposium Series 518", edited by D. W. Tedder and F. G. Pohland, American Chemical Society, Washington D.C., 1993, pp. 119-136.
- G. Crini, P. M. Badot, *Prog. Polym. Sci.*, **33**, 399 (2008).
- G. Annadurai, *Iran. Polym. J.*, **11**, 237 (2002).
- H. K. No, S. P. Meyers, *Rev. Environ. Contam. Toxicol.*, **163**, 1 (2000).
- A. Bhatnagar, M. Sillanpää, *Adv. Colloid Interfac. Sci.*, **152**, 26 (2009).
- W. S. Wan Ngah, L. C. Teong, M. A. K. M. Hanafiah, *Carbohydr. Polym.*, **83**, 1446 (2011).
- A. Srinivasan, T. Viraraghavan, *J. Environ. Manag.*, **91**, 1915 (2010).
- M. A. Nawi, S. Sabar, A. H. Jawad, Sheilatina, W. S. Wan Ngah, *Biochem. Eng. J.*, **49**, 317 (2010).
- E. Guibal, E. Touraud, J. Roussy, *World J. Microbiol. Biotechnol.*, **21**, 913 (2005).
- G. Sreelatha, V. Ageetha, J. Parmar, P. Padmaja, *J. Chem. Eng. Data*, **56**, 35 (2011).

- <sup>14</sup> A. Szygula, E. Guibal, M. Ruiz, A. M. Sastre, *Colloid. Surf. A: Physicochem. Eng. Aspects*, **330**, 219 (2008).
- <sup>15</sup> J. Barron-Zambrano, A. Szygula, M. Ruiz, A. M. Sastre, E. Guibal, *J. Environ. Manag.*, **91**, 2669 (2010).
- <sup>16</sup> K. Z. Elwakeel, *J. Hazard. Mater.*, **167**, 383 (2009).
- <sup>17</sup> V. Singha, A. K. Sharma, D. N. Tripathi, R. Sanghi, *J. Hazard. Mater.*, 161, 955 (2009).
- <sup>18</sup> N. M. Mahmoodi, R. Salehi, M. Arami, H. Bahrami, *Desalination*, **267**, 64 (2011).
- <sup>19</sup> R. Salehi, M. Arami, N.M. Mahmoodi, H. Bahrami, S. Khorramfar, *Colloid. Surf. B: Biointerfaces*, **80**, 86 (2010).
- <sup>20</sup> M.-H. Liu, S.-N. Hong, J.-H. Huang, H.-Y. Zhan, *J. Environ. Sci.*, **17**, 212 (2005).
- <sup>21</sup> E. S. Dragan, M. M. Perju, M. V. Dinu, *Carbohydr. Polym.*, **88**, 270 (2012).
- <sup>22</sup> S. Lagergren, *Kungliga Svenska Vetenskapsakademiens Handlingar*, **24**, 1 (1898).
- <sup>23</sup> Y. S. Ho, G. McKay, *Process Safety Environ. Prot.*, **76**, 183 (1998).
- <sup>24</sup> F.-C. Wu, R.-L. Tseng, R.-S. Juang, *Chem. Eng. J.*, **150**, 366 (2009).
- <sup>25</sup> W. J. Weber, J. C. Morris, *J. Sanit. Eng. Div.*, **89**, 31 (1963).
- <sup>26</sup> T. Onofrei, V. Dulman, M. Spiridon, *Analele stiintifice ale Universitatii "Al. I. Cuza" Iasi, Seria Chimie*, **2**, 191 (2002).
- <sup>27</sup> L. A. W. Tan, A. I. Ahmad, B. H. Hameed, *J. Hazard. Mater.*, **154**, 337 (2008).
- <sup>28</sup> C. Y. Shiau, C. C. Pan, *Sep. Sci. Technol.*, **39**, 1733 (2004).
- <sup>29</sup> W. H. Cheung, Y. S. Szeto, G. McKay, *Bioresource Technol.*, **98**, 2897 (2007).
- <sup>30</sup> K. Y. Foo, B. H. Hameed, *Chem. Eng. J.*, **156**, 2 (2010).
- <sup>31</sup> G. McKay, H. S. Blair, J. R. Gardner, *J. Appl. Polym. Sci.*, **27**, 3043 (1982).
- <sup>32</sup> M. Grindea, T. Forst, A. Hanganu, "Tehnologia vopsirii și imprimării textilelor" ("Textile dyeing and printing technology"), Ed. Tehnică, Bucharest, Romania, 1983.
- <sup>33</sup> J. H. Cho, D. M. Lewis, *Color. Technol.*, **118**, 198 (2002).
- <sup>34</sup> N. Sekhar, D. S. Deulgaonkar, *Colourage*, **53**, 82 (2006).
- <sup>35</sup> L. Zhou, J. Jin, Z. Liu, X. Liang, C. Shang, *J. Hazard. Mater.*, **185**, 1045 (2011).
- <sup>36</sup> S. Chatterjee, B. P. Chatterjee, A. R. Das, A. K. Guha, *J. Colloid Interfac. Sci.*, **288**, 35 (2005).
- <sup>37</sup> R. A. A. Muzzarelli, B. Muzzarelli, in "Polysaccharides. Structural diversity and functional versatility", edited by S. Dumitriu, Marcel Dekker, Hong-Kong, 1998, pp. 580.
- <sup>38</sup> N. Sakkayawong, P. Thiravetyan, W. Nakbanpote, *J. Colloid Interfac. Sci.*, **286**, 36 (2005);
- <sup>39</sup> M. Wawrzekiewicz, Zb. Hubicki, *J. Hazard. Mater.*, **172**, 868 (2009);
- <sup>40</sup> J. Gao, Q. Zhang, K. Su, R. Chen, Y. Peng, *J. Hazard. Mater.*, **174**, 215 (2010);
- <sup>41</sup> G. Bayramoğlu, M. Yakup Arica, *J. Hazard. Mater.*, **143**, 135 (2007).